NUMERICAL ASSESSMENT OF THE EFFECT NANOFLUIDS ON THE EROSION AND CORROSION IN THE RADIATOR PIPES BY USING COOLANT FLUIDS

Asifa Mahdi Mohammed / Lecturer
Electro mechanical. Eng. Dept , / University of Technology
E– mail: Asafaimahdee@yahoo.com,

ABSTRACT :-

This paper presents a numerical study of the effect nanofluids on the erosion corrosion in the pipes by using coolant fluids. One type of nanoparticles used in this paper cupper (Cu) and the base fluid (distilled water) as well as the nanoparticles size used are ranging from (20 – 50 nm). The concentrations of nanofluid used are ranging from (1 – 3 vol %). The results indicated that property of nanoparticles and their effects on the behavior of the erosion and corrosion due to the cavitation phenomenon, which causes pipe wall erosion. This study reveal the effect of the nanoparticles concentration on the flow phenomenon. Furthermore, the type and size nanoparticles play an important role in the nanofluid flow, thermall properties and erosion – corrosion behavior. The obtained results indicated that the contribution of the temperature enhancement and the velocity of nanofluids on the radiator shape, design and materials. Results showed the critical pressure distribution along the flow field and predictions on effect of temperature during the erosion – corrosion process. Moreover the results indicated the effect of velocity, temperature and thermo physical properties on on the erosion corrosion in the pipe. Two the flow condition used in this study laminar and turbulent

Keywords: Nanofluids, radiator, erosion – corrosion process, nanoparticles concentration

التقييم العددي لتأثير الموائع النانوية على تأكل التعرية الأنابيب المبردة باستخدام موائع التبريد

عاصفه مهدي / مدرس

قسم الهندسة الكهروميكانيكية / الجامعة التكنولوجية

الخلاصة :-

يقدّمُ هذ البحث دراسةَ عددية للتأثير الموائع النانوية على تآكل التعرية صدأ الأنابيب باستخدام موائع التبريد. تم في هذه الدراسة استخدام نوع واحد من الجزئيات النانوية وهو النحاس مع الماء المقطر بالإضافة الى حجم حبيبي يتراوح مابين (20 – 50 nm) و مدى تراكيز حجمية يتراوح مابين (1 – 3 vol %) حيث تم استعمال مائع نانوي مثل النحاس مع الماء المقطر . بينت النتائج ان خاصية الدقائق النانوية وتأثيرها على سلوك التأكل التعرية بسب ظاهرة تكوين الفجوات والتي تسبب تآكل جدار الأنبوب ، وهذه الدراسة تبين تأثير تركيز الدقائق النانوية على ظاهرة التدفق. علاوة على ذلك ، ان نوع وحجم الدقائق النانوية يلعب دورا هاما في تدفق الموائع النانوية ، والخواص الحرارية وكذلك سلوك تعرية وتأكل في الانابيب. اشارت النتائج على مساهمة زيادة درجة الحرارة وسرعة المواد النانوية على شكل المبرد والتصميم والمواد. وبينت النتائج توزيع الضغط الحرج على طول مجال تدفق والتنبؤات حول تأثير درجة الحرارة على عملية تأكل التعرية. اضافة الى ذلك بينت تأثير السرعة ودرجة الحرارة والخواص الحرارية على سلوك تأكل التعرية في انابيب التبريد. تم في هذه الدراسة استخدام حالتين الجريان الطباقي والجريان المضطرب .

الكلمات المفتاحية: المائع النانوي ، المبرد ، عملية تعرية وتأكل ، تركيز الجزئيات النانوية .

NOMENCLATURE :-

Symbol	Quantity	units
Kn	Thermal conductivity of nanofluid	$W/m^2 K$
Kp	Thermal conductivity of nanoparticles	$W/m^2 K$
Kb	Thermal conductivity of nanoparticles	—
Q	thermal energy	J
Cp	Specific heat	J/kg K
h	heat transfer coefficient	$W/m^2 K$
$\dot{m}$	Mass flow rate	kg/s
Nu	Nusselt number	—
Pr	Prandtl number $= \frac{\mu}{\rho\ \alpha}$	—
Re	Reynolds number $= \frac{4\dot{m}}{\pi\ dhy\ \mu}$	—
T	Temperature	°C
	Greek Symbol	
μ	Dynamic viscosity	$N.s/m^2$
ρ	density	Kg/m^3
Φ	Volume concentration	—
β	Thermal expansion coefficient	
	Subscripts	
bf	Base fluid	—
nf	Nanofluid	—
in	input	—
out	output	—
w	wall	—

1- INTRODUCTION :-

In the oil and gas trade, the raw created fluids extracted from reservoirs sometimes contain solid particles like sands, cuttings and additives. Erosion of fabric surfaces ensuing from the impact of those solid particles will injury several piping devices and limit the reliable operation of piping systems. Solid particle erosion may be much overpriced, which can need parts to be overtimes repaired or replaced. Additionally, part failure leads to overpriced system shutdowns, inflicting loss of valuable production revenue. to stay the piping system operative safely and to reduce the loss caused by solid particle erosion, associate degree correct erosion prediction technique is required. This can facilitate estimate the service life and predict the erosion pattern and site within the pure mathematics wherever severe erosion is probably going to occur. Whereas solid particle erosion may be a complicated method and therefore the particles get momentum from encompassing carrier fluid; the momentum of particles carries them across streamlines; and therefore the particles impinge the wall of the fittings leading to erosion injury. The severity of abrasion injury may be determined by several factors, like production flow rates, fluid properties, particle production rates, particle properties, particle size, instrumentality and piping wall materials. Hence, most of the empirical models, **Salama [1983], Bourgoyne [1989], Shirazi [1995], Det Norske [2007]** cannot account for the full method and solely work well among limits. The numerical simulation show distinct advantages compared to the empirical models during this respect. Since the first 1990s, process fluid dynamics (CFD) has been wide used for analyzing solid particle erosion. **Mclaury [1996]** developed a CFD – primarily based generalized erosion prediction procedure to account for erosion ensuing from each direct and random impingement and incontestable its pertinence to some two dimensional pure mathematics. **Wang [1997]** used flow modeling and particle trailing to analyze the results of two-dimensional elbow curvature on erosion rates. **Forder et al**. **[1998]** bestowed a CFD – primarily based erosion model to predict the erosion rates in field management valves. **Edwards [2000]** enforced a comprehensive erosion prediction procedure under consideration general 3D geometries and foretold erosion in many fittings like elbows, plug tees, unforeseen contractions and unforeseen expansions. **Chen et al. [2001]** added a random rebound model and investigated the relative erosion severity in elbows and plug tees. **Zhang et al. [2009]** changed the particle motion within the near – wall region and improved the particle trajectories once impact. CFD primarily based erosion modeling consists of three primary steps: flow modeling, particle trailing and erosion prediction. Each step ought to be verified to make sure the effectiveness of numerical simulation. In the present work, relative theories and process models for every step are mentioned intimately here in. Flow modeling is that the basic a part of the excellent procedure to simulate the flow field in geometries. The flow structure plays a major role not solely within the mechanical phenomenon behavior of solid particles however additionally within the style of impingement that happens. Many turbulent models are developed to resolve the Reynolds averaged Navier

– Stokes equations, that are applicable severally for various flow conditions. **Edwards [2000]** mentioned the capabilities of three classic turbulent models with two – dimensional simulations. **Chen [2004]** evaluated the accuracy of flow modeling applied to a liquid pipe flow. In the present work, flow simulations area unit performed in a very ninety degree elbow for gas pipe flow and therefore the results are compared with experimental knowledge on the market within the literature to judge the accuracy of flow modeling. within the second step, particles carried by close fluids are half-tracked to work out the impact location, speed and angle. A Lagrange approach is chosen to predict the mechanical phenomenon, during which the fluid is treated as a time and therefore the particles act as one object within the fluid. Naturally, the particles submerged in carrier fluid may also have an effect on the flow field conversely. In the oil and gas production, the sand concentration is fairly little in order that the result of sand particles on the carrier fluid is assumed negligible **Chen [2004]**. In fact this hypothesis is accepted by most researchers, **Mclaury [1996], Wang [1997], Forder et al**. **[1998], Edwards [2000], Chen et al. [2001], Zhang et al. [2007A], Chen [2004], Zhang [2006]**. However, particles will compile specially areas of flow filed even on low level of sand concentration for a few reasons, in order that the counteractive to fluids shouldn't be neglected. The interaction between particles and fluids is analyzed within the present work. By examination with experimental information, two interactive patterns named absolutely coupling and a technique coupling are mentioned. The third step of the CFD – primarily based erosion prediction procedure is to calculate the erosion caused by solid particle impingements. it's a fancy method that the fabric is far from the inner surface as a results of continual impact of solid particles whereas it's inessential to explore the microstructure mechanism, some empirical equations will give spare accuracy in predicting the megascopic erosion results. It's noted that the erosion results expected by the E/CRC erosion equation and also the Oka et al. erosion equation were ever compared by **Zhang et al [2006B]**. In the present work, four classic erosion equations developed by E/CRC (Erosion/Corrosion Research Center) **Zhang et al [2006B]**, **DNV Det Norske [2007]**, **Oka et al. [2005]**, **Yoshida et al. [2005]** and **Grant** and **Grant [1973]** are introduced to calculate the penetration rates.

1. PHYSİCAL PROBLEM DEFİNİTİON :

a.Coolant System Fluids

Fluids heating and cooling play important roles in many industries including power stations, production processes, transportation and electronics. Fluids, such as water, ethylene glycol and engine oil have poor heat transfer performance and therefore high compactness and effectiveness of heat transfer systems are necessary to achieve the required heat transfer. Among the efforts for enhancement of heat transfer the application of additives to liquids is noticeable,**Bergles [1973]**.

2. Erosıon-Corrosıon Behavior ("Flow-Assisted" or "Flow-Accelerated" Corrosion)

An increase in corrosion brought about by a high relative velocity between the Corrosive environment and the surface, **Derek [2008]**.

Removal of the metal may be:

- As corrosion product which "spalls off" the surface because of the high fluid shear and bares the metal beneath.
- As metal ions, which are swept away by the fluid flow before they can deposit as corrosion product – remember the distinction between erosion – corrosion and erosion:

Erosion is the straightforward wearing away by the mechanical abrasion caused by suspended particles, e.g. sand – blasting, erosion of turbine blades by droplets. Erosion and corrosion also involves a corrosive environment the metal undergoes a chemical reaction. Figure (1) indicated high speed jet of fluid impact on a fixed surface. Figure (1) reveals the pitting corrosion of tube wall

In the present work, the study will investigate numerically the flow behavior of suspension of (Cu) nanoparticles in base fluid (water) inside radiator system pipes as indicated in the figure (3) by using STAR – CCM +. The effect of nanomaterials properties and their effects on the Erosion – corrosion, it was studied. In order to emphasizes the enhancement of the thermal behaviour due to the nanoparticles presence in the base fluid. Also, to investigate the flow behavior of such fluids and the effect of velocity distribution which cause extra penalty in pumping power in the laminar flow.

3. MATHEMATICAL MODEL AND GOVERNING EQUATIONS OF FLUID MOTION :

The mechanical properties can be estimated by using the following forms. The thermal conductivity of the nanofluid can be calculated from ,**Hamilton[1962]** using the following equation:

$$k_{nf} = \frac{k_p+(n-1)k_b-(n-1)(k_b-k_p)\Phi}{k_p-(n-1)k_b+(k_b-k_p)\Phi} \quad (1)$$

Where: k_{nf} is the thermal conductivity of the nanofluid, k_p is the thermal Conductivity of the nanoparticle, k_b is the thermal conductivity of the base fluid, Φ is the volume fraction of nanoparticles in the suspension (phase change), and n is the shape factor depend on the partical shape (phase change), n equals to 3 for spherical nanoparticles.

The density, viscosty, specific heat and thermal expansion coefficient can be found by using the following forms respectively, **Yang [2005].**

$$\rho_{nf} = \rho_p\Phi + (1-\Phi)\rho_b \quad (2)$$

$$\mu_{nf} = (1+2.5\Phi)\mu_b \quad (3)$$

$$Cp_{nf} = \left[\frac{(1-\Phi)(\rho cp)_b+\Phi(\rho cp)_p}{(1-\Phi)\rho_b+\Phi\rho_p}\right] \quad (4)$$

$$\beta_{nf} = \left[\frac{1}{1+\frac{(1-\Phi)\rho_b}{\Phi\rho_p}}\frac{\beta_p}{\beta_b}+\frac{1}{1+\frac{\Phi\ \rho_p}{1-\Phi\rho_b}}\right]\beta_b \quad (5)$$

- Continuity equation

$$\frac{\partial r u_r}{\partial r} + \frac{\partial u_\theta}{\partial \theta} = 0 \quad (6)$$

- Momenum equations (r, θ and x)

$$\rho_{nf}\left(u_r\frac{\partial u_r}{\partial r} + \frac{u_\theta}{r}\frac{\partial u_r}{\partial \theta} - \frac{u_\theta^2}{r}\right) = -\frac{\partial p}{\partial r} + \mu_{nf}\left(\frac{\partial^2 u_r}{\partial r^2} + \frac{1}{r}\frac{\partial u_r}{\partial r} + \frac{1}{r^2}\frac{\partial^2 u_r}{\partial \theta^2} - \frac{u_r}{r^2} - \frac{2}{r^2}\frac{\partial u_\theta}{\partial \theta}\right) + \rho_{nf} g_r \quad (7)$$

$$\rho_{nf}\left(u_r\frac{\partial u_\theta}{\partial r} + \frac{u_\theta}{r}\frac{\partial u_\theta}{\partial \theta} + \frac{u_r u_\theta}{r}\right) = -\frac{1}{r}\frac{\partial p}{\partial \theta} + \mu_{nf}\left(\frac{\partial^2 u_\theta}{\partial r^2} + \frac{1}{r}\frac{\partial u_\theta}{\partial r} + \frac{1}{r^2}\frac{\partial^2 u_\theta}{\partial \theta^2} + \frac{2}{r^2}\frac{\partial u_r}{\partial \theta} - \frac{u_\theta}{r^2}\right) + \rho_{nf} g_\theta \quad (8)$$

$$\rho_{nf}\left(u_r\frac{\partial u_x}{\partial r} + \frac{u_\theta}{r}\frac{\partial u_x}{\partial \theta}\right) = -\frac{\partial p}{\partial x} + \mu_{nf}\left(\frac{\partial^2 u_x}{\partial r^2} + \frac{1}{r}\frac{\partial u_x}{\partial r} + \frac{1}{r^2}\frac{\partial^2 u_x}{\partial \theta^2}\right) + \rho_{nf} g_x \quad (9)$$

- Energy equation

$$\rho_{nf} Cp_{nf}\left(u_r\frac{\partial T}{\partial r} + \frac{u_\theta}{r}\frac{\partial T}{\partial \theta} + u_x\frac{\partial T}{\partial x}\right) = k_{nf}\left(\frac{\partial^2 T}{\partial r^2} + \frac{1}{r}\frac{\partial T}{\partial r} + \frac{1}{r^2}\frac{\partial^2 T}{\partial \theta^2}\right) \quad (10)$$

By using the dimensionless forms as shown below:-

- Prandtl number $(Pr) = \frac{Cp_{nf}\,\mu_{nf}}{k_{nf}}$
- Reynolds number $(Re) = \frac{\rho_{nf}\, d\, u}{\mu_{nf}}$
- Grashof number $(Gr) = \frac{g\beta_{nf}(T_w - T)d3}{\vartheta_{nf}^2}$

Where : d and r the diameter and the radius of the tube, (u) the velocity of the nanofluid, (ϑnf) the kinematic viscosity of the nanofluid , (β_{nf}) thermal expansion coefficient of the nanofluid. The cylindrical form of the Navier – Stokes and energy equations, can be written based on the Oberbeck – boussinesq approximation and by using the dimensionless parameters:

- Momenum equations (r, θ and x) respectively

$$u_r\frac{\partial u_r}{\partial r} + \frac{u_\theta}{r}\frac{\partial u_r}{\partial \theta} - \frac{u_\theta^2}{r} =$$

$$-\frac{\partial p}{\partial r} + \frac{1}{Re}\left(\frac{\partial^2 u_r}{\partial r^2} + \frac{1}{r}\frac{\partial u_r}{\partial r} + \frac{1}{r^2}\frac{\partial^2 u_r}{\partial \theta^2} - \frac{u_r}{r^2} - \frac{2}{r^2}\frac{\partial u_\theta}{\partial \theta}\right) - \frac{u_x^2}{r sin\theta}\, sin\theta + \frac{Gr}{Re^2}\, T cos\theta \quad (11)$$

$$u_r\frac{\partial u_\theta}{\partial r} + \frac{u_\theta}{r}\frac{\partial u_\theta}{\partial \theta} - \frac{u_r u_\theta}{r} =$$

$$-\frac{1}{r}\frac{\partial p}{\partial \theta} + \frac{1}{Re}\left(\frac{\partial^2 u_\theta}{\partial r^2} + \frac{1}{r}\frac{\partial u_\theta}{\partial r} + \frac{1}{r^2}\frac{\partial^2 u_\theta}{\partial \theta^2} + \frac{2}{r^2}\frac{\partial u_r}{\partial \theta} - \frac{u_\theta}{r^2}\right) - \frac{u_x^2}{r sin\theta}\, cos\theta + \frac{Gr}{Re^2}\, T sin\theta \quad (12)$$

$$u_r \frac{\partial u_x}{\partial r} + \frac{u_\theta}{\mathrm{r}} \frac{\partial u_x}{\partial \theta} = -\frac{\partial \mathrm{p}}{\partial \mathrm{x}} + \frac{1}{Re}\left(\frac{\partial^2 u_x}{\partial r^2} + \frac{1}{\mathrm{r}} \frac{\partial u_x}{\partial r} + \frac{1}{\mathrm{r}^2} \frac{\partial^2 u_x}{\partial \theta^2}\right) \quad (13)$$

- Energy equation

$$u_r \frac{\partial T}{\partial r} + \frac{u_\theta}{\mathrm{r}} \frac{\partial T}{\partial \theta} + u_x \frac{\partial T}{\partial x} = \frac{1}{Re\, Pr}\left(\frac{\partial^2 T}{\partial r^2} + \frac{1}{\mathrm{r}} \frac{\partial T}{\partial r} + \frac{1}{\mathrm{r}^2} \frac{\partial^2 T}{\partial \theta^2}\right) \quad (14)$$

4. SOLVING BY STAR – CCM + PROGRAM :

In the present work the problem is assumed to be three dimensional, steady, incompressible and Newtonian laminar and turbulent fluid flow. Also the thermal interaction between the Nanofluid and the pipe surface takes place under the assumption of segregated fluid temperature.

Boundary conditions

The Nanofluid properties can be estimated by defining the properties as shown in the Table (1) Where ρ, Cp, k and μ are density, specific heat, thermal conductivity and viscosity respectively. In addition, the initial condition of the Nanofluid velocity and temperature can be defined by applying nanofluid velocity (u=0.05 m/s) for laminar flow and (u=0.5 m/s) for turbulent flow and the inlet nanofluid temperature (350 K) as well as daimeter of the tube (d= 10mm). Copper nanoparticles suspended in water with base size diameter (20 – 50) nm and with concentration of 1, 2 and 3% in the base fluid.

RESULTS AND DISCUSSION :

In some engineering applications the cavitation is major reason for wear cyclic stress throughout recurrent implosion and thus voids of collapsing happens on the subject of surface of metal for this reason. These results indicated that the wear of the metal inflicting cavitation. This type of wear was happens in pump impellers and bends because of fulminant modification within the direction of liquid. The cavities result to rapid changes of liquid pressure wherever the pressure is comparatively low. The upper liquid pressure will generate associate degree intense blast wave and also the voids founder. Adding the nanoparticles to the bottom fluid can cut back cavitation development, wherever reduce the void or bubbles result in decreases the pressure, therefore reducing cavitation development. Once the important pressure can happen the cavitation development and this parameter can determined this development furthermore as pumping method that causes this development [21]. By applying eqs. 1, 2, 3 and four the properties of the nanofluid may be obtained as shown within the Table (2). This study together with 2 forms of the pipes the primary longitudinal pipe whereas the second U – bend pipes within the bedded and flow. Fig (4) pictured the longitudinal pipe within the geometry and mesh generation for laminar and turbulent flow. Figs (5 – 18) shows velocity magnitude and vector, temperature distribution and outlet face temperature distribution, outlet face velocity magnitude and vector for laminar and flow. Velocity and temperature are depicted as contours, and it shows that the distinction between

minimum and also the most values of temperature is trusted velocity inlet. Erosion and corrosion is caused by the relative movement between a corrosive fluid and a metal surface. The mechanical facet of the movement is vital and friction and wear phenomena may be concerned. This method leads to the formation of grooves, valleys, wavy surfaces, holes, etc.

Corrosion is special kind of erosion attributable to "implosion of gas bubbles on surface of metal referred to as cavitation. it always related to variations of sudden in pressure that relating to with the hydrodynamic parameters of the fluid (e.g. hydraulic rotary engine blades, propellers, stirrer blades, etc.). The regime of hydraulic is extremely necessary within the fluid. The condition of the nice surface decreases the potential sites variety to the vapor bubbles forming. In most cases the rise of fluid pressure comfortable to keep up one part fluid to avoiding the formation of vapor bubbles. The phenomena of turbulence will destruction protecting films and cause high the rates of corrosion what is more extremely resistant from static conditions. On the opposite hand within the streamline flow regime, the rate of fluid flow contains a variable result looking on the material involved.

In addition the results show the rate (vectors and Magnitudes) on the inlet and outlet faces for each longitudinal and U – bend pipes within the laminar and flow. Figs (11 – 12) reveal center line velocity distribution and center line pressure distribution in streamline flow. This figures indicated that the rate will increase with position whereas pressure decrease with position as a result of once fluid passes over a solid body, the streamlines meet up with a long, the flow velocity will increase, and therefore the pressure decreases. Influence of fluid properties and temperature on pump cavitation performance these parameters important in cavitation development. The Tables (3) and (4) indicated that the result of nanoparticles concentration on pressure drop, inlet and outlet temperature also as temperature distinction to the laminar and flow with longitudinal tube. Figs (19) represented the U – bend pipe within the pure mathematics and mesh generation for laminar and turbulent flow. Figs (20 – 31) shows speed magnitude and vector, water and outlet face velocity vector and magnitude, temperature distribution, water and outlet face temperature distribution for laminar and flow. The Tables (5) and (6) indicated that the result of volume concentration on pressure drop, water and outlet temperature and distinction temperature for laminar and flow with U – bend pipe. The leads to tables (7 – 10) reveal the longitudinal and U – bend pipe for laminar and flow. This Tables indicated that the result of volume concentration on Reynolds range, mass flow, convection heat transfer, heat, coefficient of heat transfer and Nassult number. The dimensionless range pressure coefficient will be calculable so as to describe the relative pressures throughout a flow field:

$$Cp = \frac{\Delta p}{\frac{1}{2}\rho u^2} \qquad (15)$$

In order to calculate the heat transfer between a moving fluid and the pipe wall, Nassult number can be obtain by using the relation:

$$Nu = \frac{hD}{k} \quad (16)$$

Where h can be obtained by using the convection heat transfer equation:

$$Q = hA(\Delta T) \quad (17)$$

And

$$Q = \dot{m}\, Cp\, \Delta T \quad (18)$$

6. CONCLUSIONS :-

The present work can demonstrate the following points:-

1. Adding the nanoparticles will reduce cavitation phenomenon.
2. Properties of nanomaterials and their effects on the erosion – corrosion behavior due to the cavitation phenomenon, which causes pipe wall erosion.
3. The impact of nanoparticles concentration very important factor in the flow phenomenon as well as type, shape, size and thermal properties.
4. The distribution of the critical pressure along the flow field play important role in fluid flow.
5. The contribution of the temperature improvement and velocity flow within the radiator through the shape, design and materials.

Table (1) properties of base fluid and nanoparticles, Hamilton [1996] and Yang [2005]

Physical properties of fluid and nanoparticles		
Physical properties	Cu	Water
Cp (J/kg.K)	385	4191.8
ρ (kg/m^3)	8954	973
K (W/m.K)	390	0.668
μ (kg/m.s)	——	3.72 *10^{-4}

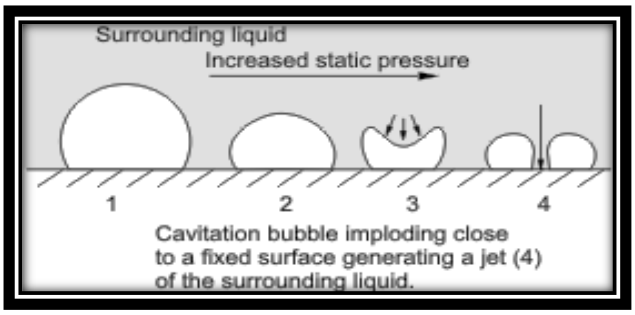

Fig.1. High speed jet of fluid impact on a fixed surface

Fig.2. Pitting corrosion of tube wall,

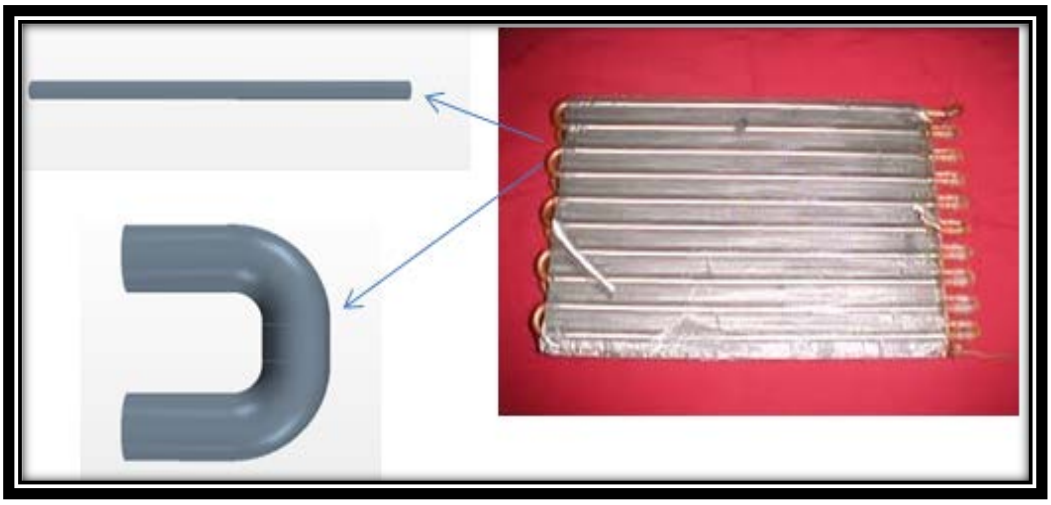

Fig. 3. Sample of radiator pipes

Table (2)

Ø	k_{nf}	ρ_{nf}	Cp_{nf}	μ_{nf}
1% Cu	1.0374	1052.81	3868.04	$3.813*10^{-4}$
2% Cu	1.0683	1132.62	3589.9	$3.906*10^{-4}$
3% Cu	1.1	1212.43	3348.39	$3.999*10^{-4}$

For Longitudinal Pipe φ=1%vol

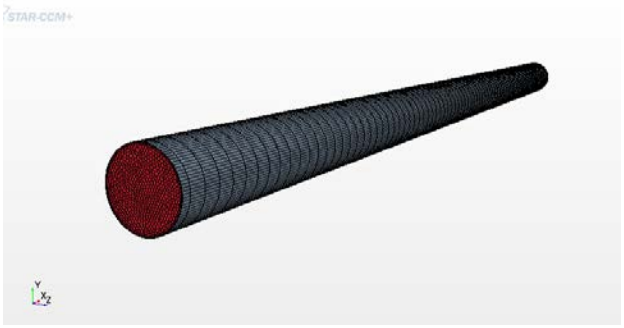

Fig. 4. Longitudinal Pipe (Geometry and Mesh generation)

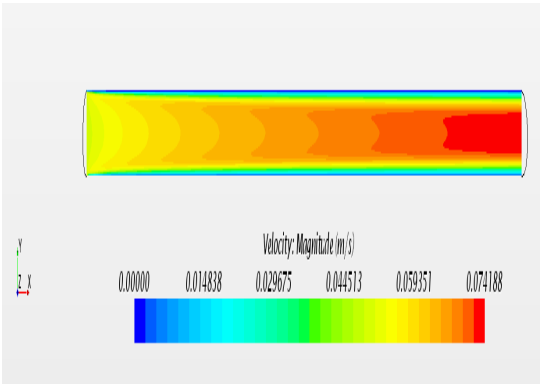

Fig. 5. Velocity Magnitude for laminar flow

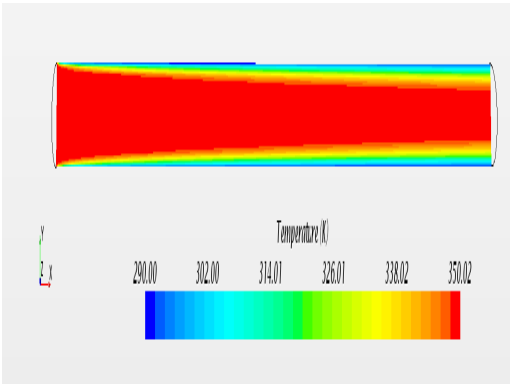

Fig. 6. Temperature Distribution in laminar flow

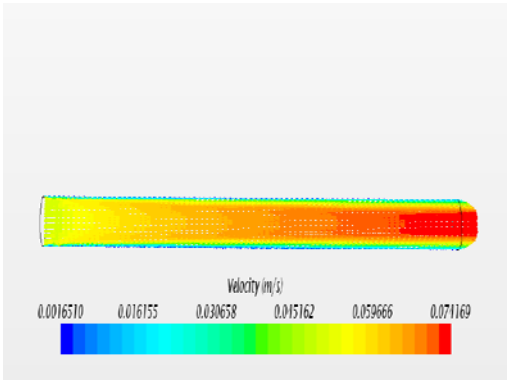

Fig. 7. Velocity Vector for laminar flow

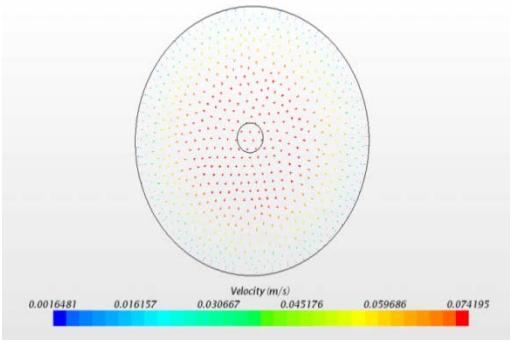

Fig.8. Outlet Face Velocity vector in laminar flow

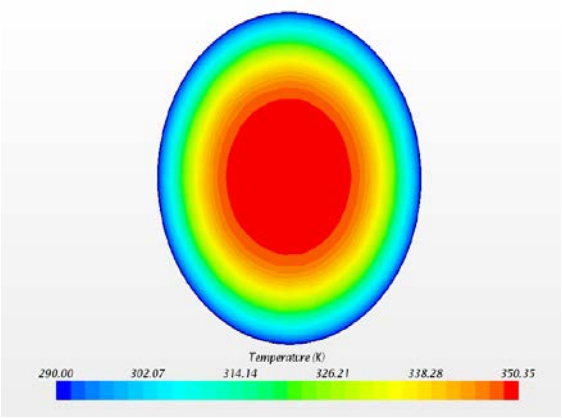

Fig. 9. Outlet Face Temperature Distribution in laminar flow

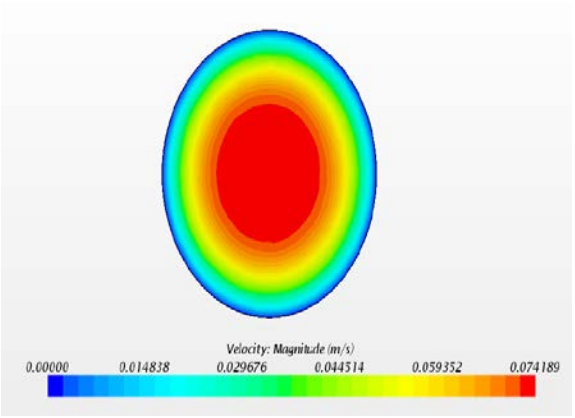

Fig. 10. Outlet Face Velocity magnitude in laminar flow

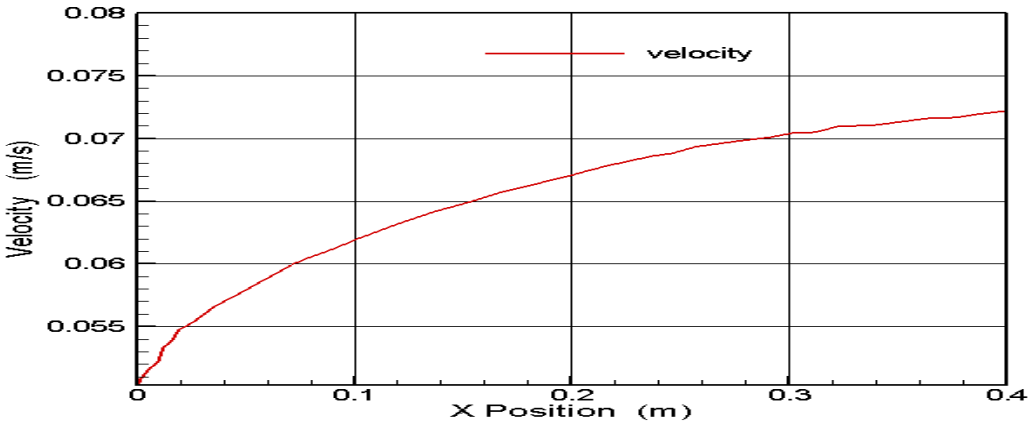

Fig. 11. Centre line velocity distribution in laminar flow

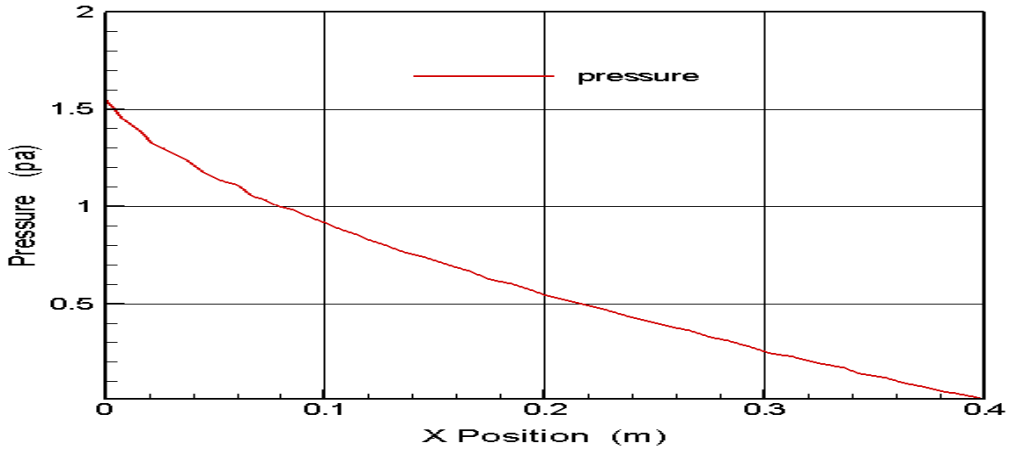

Fig. 12. Centre line pressure distribution in laminar flow

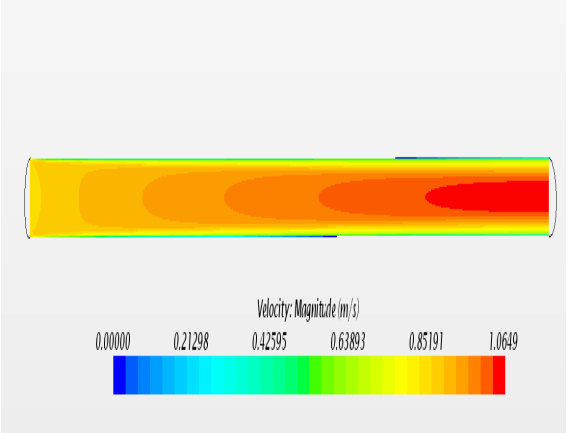

Fig. 13. Velocity Magnitude for turbulent flow

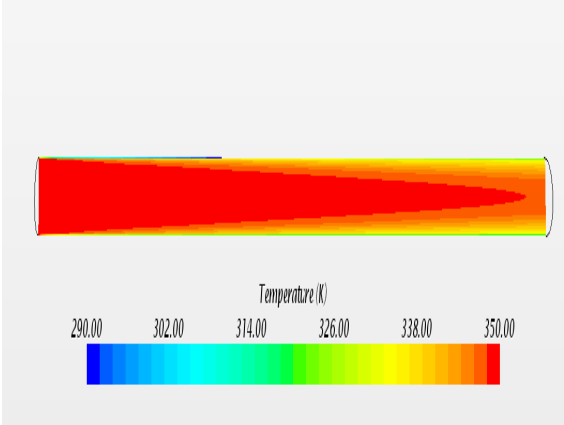

Fig. 14. Temperature distribution in turbulent flow

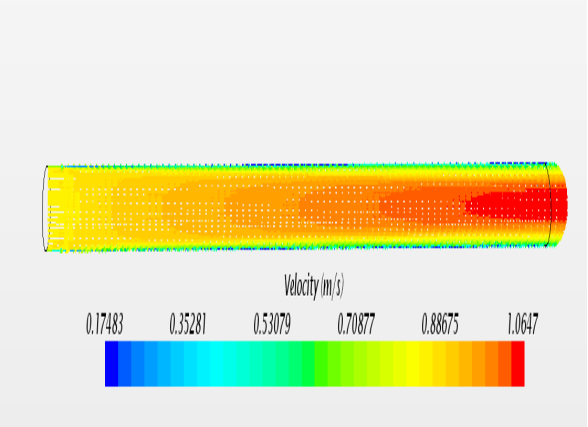

Fig. 15. Velocity vector for turbulent flow

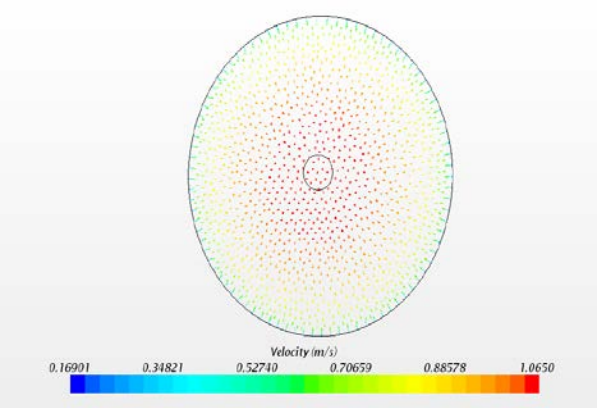

Fig. 16. Outlet Face Velocity vector in turbulent flow

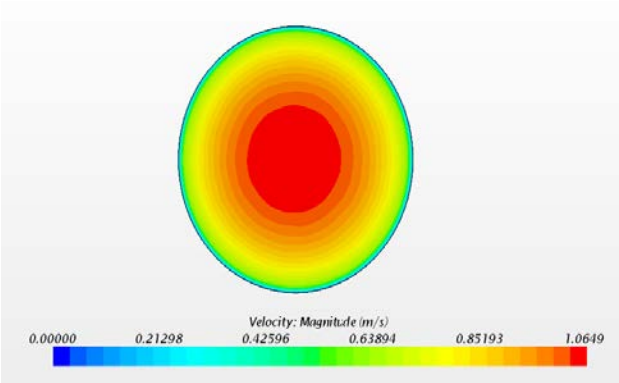

Fig. 17. Outlet Face Velocity magnitude in turbulent flow

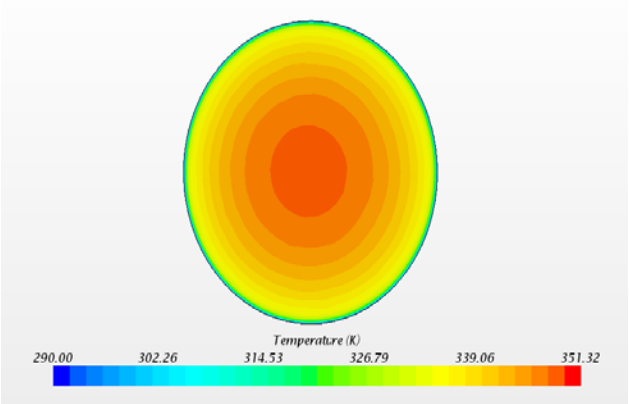

Fig. 18. Outlet Face Temperature Distribution in turbulent flow

Table (3) longitudinal pipe results for laminar flow

Ø	ΔP	T_{in}	T_{out}	ΔT
1% vol.	1.683824e+00	3.500000e+02	3.289574e+02	0.210426e+02
2% vol.	1.759915e+00	3.500000e+02	3.287614e+02	0.212386e+02
3% vol.	1.835227e+00	3.500000e+02	3.285611e+02	0.214389e+02

Table (4) longitudinal pipe results for turbulent flow

φ	ΔP	T_{in}	T_{out}	ΔT
1% vol.	8.355667e+01	3.500000e+02	3.383953e+02	0.116047e+02
2% vol.	8.914004e+01	3.500000e+02	3.380482e+02	0.119518e+02
3% vol.	9.525675e+01	3.500000e+02	3.376424e+02	0.123576e+02

For U – bend Pipe φ =1%vol.

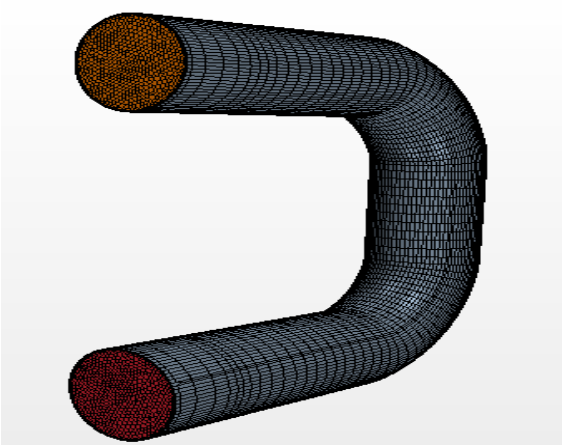

Fig. 19. U – bend pipe (Geometry and Mesh generation)

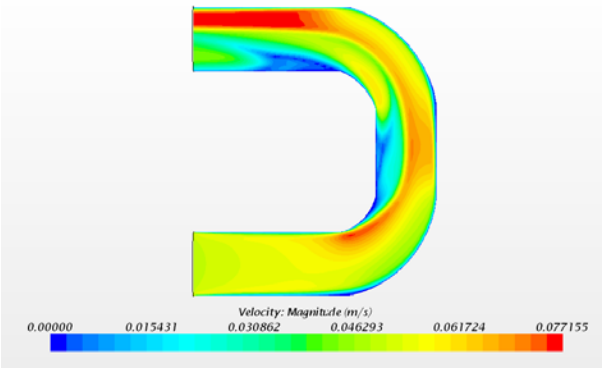

Fig. 20. Velocity Magnitude for laminar flow

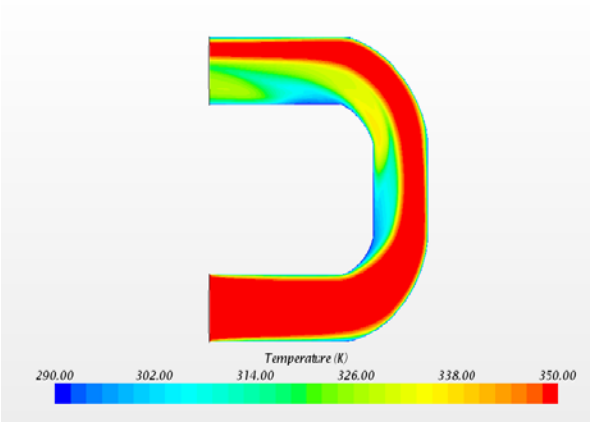

Fig. 21. Temperature Distribution in laminar flow

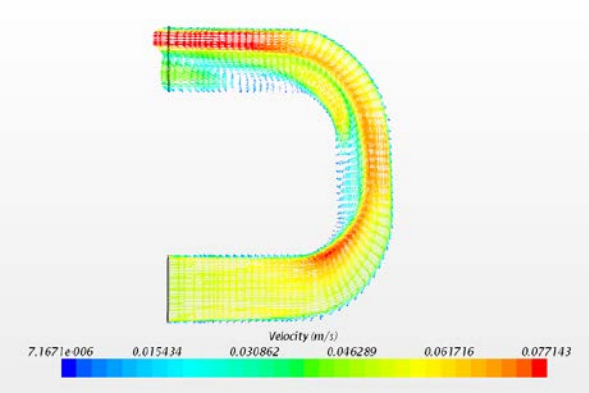

Fig. 22. Velocity vector for laminar flow

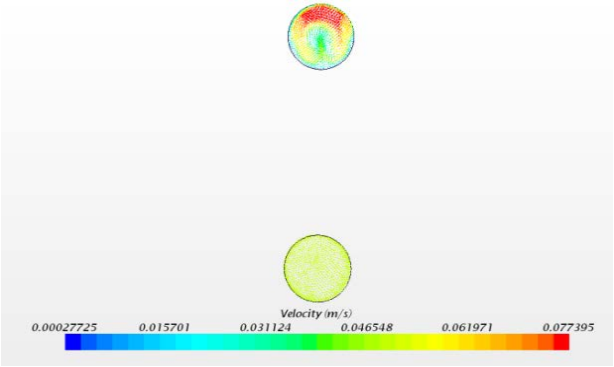

Fig. 23. Inlet and outlet face velocity vector in laminar flow

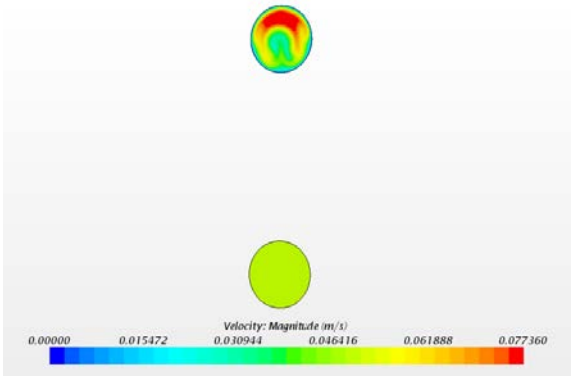

Fig. 24. Inlet and outlet face velocity magnitude in laminar flow

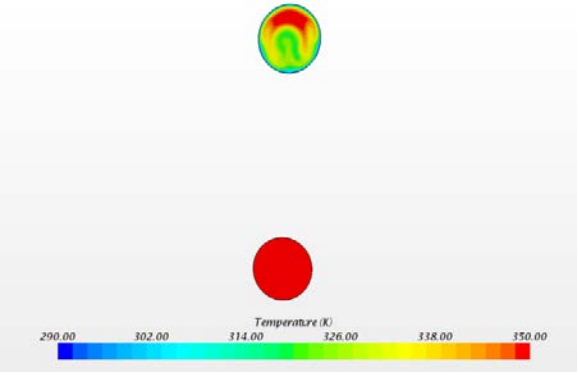

Fig. 25. Inlet and outlet face temperature distribution in laminar flow

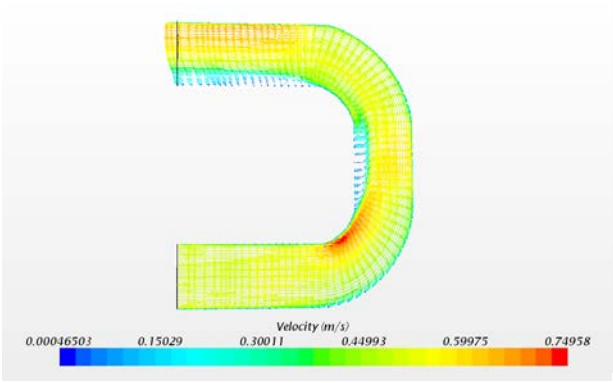

Fig. 26. Velocity magnitude for turbulent flow

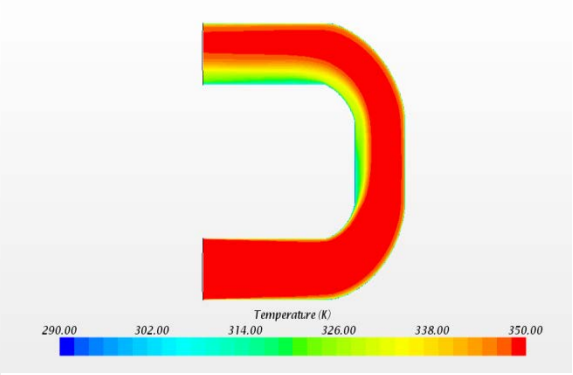

Fig. 27. Temperature distribution in turbulent flow

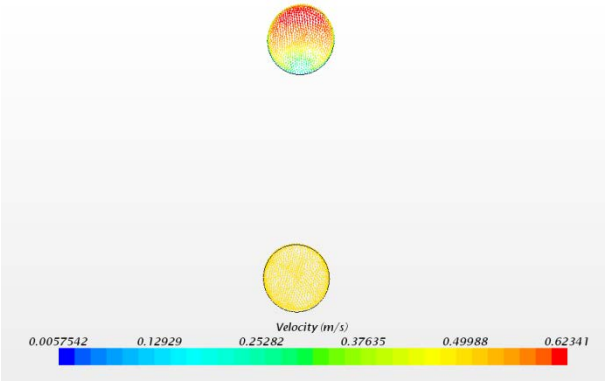

Fig. 28. Velocity Vector for turbulent flow

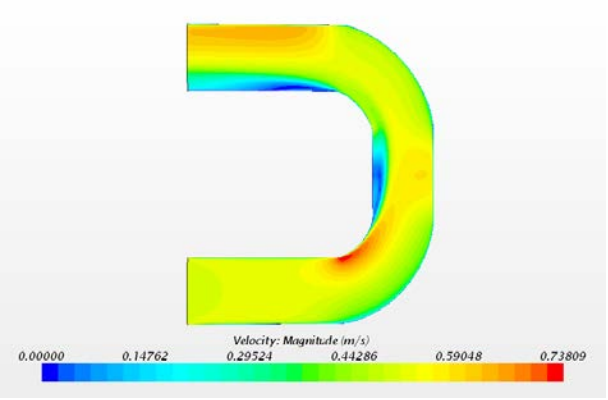

Fig. 29. Inlet and outlet face velocity vector in turbulent flow

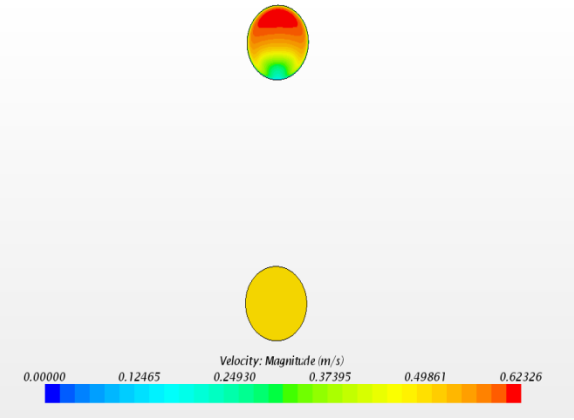

Fig. 30. Inlet and outlet faces velocity magnitude in turbulent flow

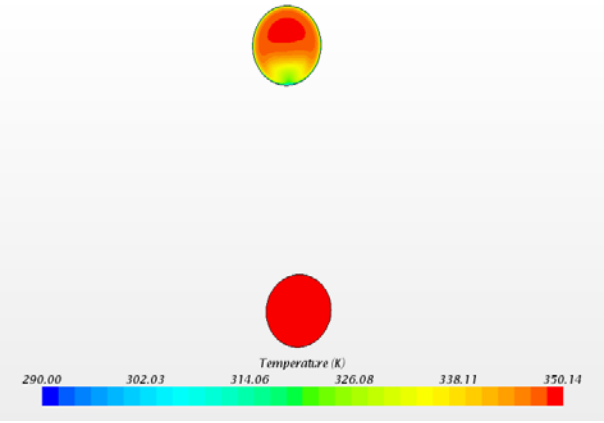

Fig. 31. Inlet and outlet faces temperature distribution in turbulent flow

Table (5) U – bend pipe results for laminar flow

Ø	ΔP	T_{in}	T_{out}	ΔT
1% vol.	1.949665e+00	3.500000e+02	3.304376e+02	0.195624e+02
2% vol.	2.055785e+00	3.500000e+02	3.301043e+02	0.198957e+02
3% vol.	2.107562e+00	3.500000e+02	3.298112e+02	0.201888e+02

Table (6) U – bend pipe results for turbulent flow

Ø	ΔP	T_{in}	T_{out}	ΔT
1% vol.	8.978510e+01	3.500000e+02	3.418567e+02	0.081433e+02
2% vol.	9.531288e+01	3.500000e+02	3.419605e+02	0.083950e+02
3% vol.	1.012314e+02	3.500000e+02	3.414700e+02	0.085355e+02

Table (7) longitudinal pipe results for laminar flow

Ø	Re	$\dot{m}$ (kg/s)	Q (W)	C_p	h (W/m^2.s)	Nu
1% vol.	1380.55	0.00413	336.1556	1.27948	445.8402	4.1199
2% vol.	1449.84	0.00444	338.5253	1.243075	448.9831	4.2027
3% vol.	1515.91	0.00476	341.700	1.210941	453.1937	4.2895

Table (8) longitudinal pipe results for turbulent flow

Ø	Re	$\dot{m}$ (kg/s)	Q (W)	C_p	h (W/m^2.s)	Nu
1% vol.	13805.53	0.04134	1855.819	0.63492	2461.356	23.5787
2% vol.	14498.46	0.04447	1908.019	0.62962	2530.588	23.6879
3% vol.	15159.96	0.04761	1970.009	0.62853	2612.80	23.7262

Table (9) U – bend pipe results for laminar flow

Ø	Re	$\dot{m}$ (kg/s)	Q (W)	C_p	h (W/m^2.s)	Nu
1% vol.	1380.55	0.00413	312.5094	1.48149	1038.142	9.7175
2% vol.	1449.84	0.00444	317.1206	1.45205	1053.460	9.861
3% vol.	1515.91	0.00476	321.7758	1.39063	1068.925	10.007

Table (10) U – bend pipe results for turbulent flow

Ø	Re	$\dot{m}$ (kg/s)	Q (W)	C_p	h (W/m^2.s)	Nu
1% vol.	13805.53	0.04134	1302.152	0.682251	4325.69	41.066
2% vol.	14498.46	0.04447	1340.201	0.673220	4452.09	41.674
3% vol.	15159.96	0.04761	1359.825	0.66795	4517.28	41.697

REFERENCES :-

A.E. Bergles, "Recent development in convective heat transfer augmentation", Appl. Mech. Rev. 26 (1973) 675–682.

Bourgoyne, A.T., “Experimental Study of Erosion in Diverter Systems Due to Sand Production”, Proceeding of SPE/IADC Drilling Conference, New Orleans, LA, SPE/IADC 18715, 1989.

Chen, X.H., “Application of Computational Fluid Dynamics (CFD) to Flow Simulation and Erosion Prediction in Single – Phase and Multiphase Flow”, Ph.D. Thesis, Department of Mechanical Engineering, Oklahoma, United States The University of Tulsa, 2004.

Chen, X.H., Mclaury, B.S. and Shirazi, S.A., “Application and Experimental Validation of a Computational Fluid Dynamics (CFD) – based Erosion Prediction Model in Elbows and Plugged tees”, Computers & Fluids, Vol. 33 (10), pp. 1251 – 1272, 2001.

Det Norske Veritas (DNV), 2011, “Erosive Wear in Piping Systems”, Recommended Practice RP-O501, Revision 4.2 – 2007.

Derek H. Lister “corrosion for engineers”. Book, chapter three, pages (1 – 3), 2008.

Edwards, J.K., "Development, Validation, and Application of a Three-Dimensional, CFD-Based Erosion Prediction Procedure", Ph.D. Thesis, Department of Mechanical Engineering, Oklahoma, United States , The University of Tulsa, 2000.

Forder, A., Thew, M. and Harrison, D, "A numerical investigation of solid particle erosion experienced within oilfield control valves", Wear, Vol. 216, pp. 184 – 193, 1998,.

Grant, G., Tabakoff, W., "An Experimental Investigation of the Erosive Characteristics of 2024 Aluminum Alloy", University of Cincinnati, Ohio,Technical Report 73 – 37, 1973.

Hamilton, R.L. and O.K. Crosser," Thermal conductivity of heterogeneous component systems". Engineering Chemistry Fundamentals, , p. 187.124, 1962.

McLaury, B.S., "Predicting Solid Particle Erosion Resulting From Turbulent Fluctuation in oil Field Geometries", Ph.D. Thesis, Department of Mechanical Engineering, Oklahoma, United States, The University of Tulsa, 1996.

Oka, Y.I., Okamura, K. and Yoshida, T., "Practical Estimation of Erosion Damage Caused by Solid Particle Impact". Part 1: Effects of Impact Parameters on a Predictive Equation", 16th International Conference on Wear of Materials, Wear, Vol. 259, pp. 95 – 101, 2005.

Shirazi, S.A., McLaury, B.S., Shadley, J.R. and Rybicki, E.F., , "Generalization of the API RP 14E Guideline for Erosive Services", Journal of Petroleum Technology, Vol. 47 (8), pp. 693 – 698, 1995.

V. Bharath Kumar1, P.Suneetha1, K.Ramakrishna Prasad2"Lubrication of Journal Bearing Consider in Thermal Effect in Couple Stress Fluid Considering Cavitation", International Journal of Advanced Research, Volume 1, Issue 2, 59 – 66, 2013.

Wang, J.R., "Modeling Flow, Erosion and Mass Transfer in Elbows", Ph.D. Thesis, Department of Mechanical Engineering, Oklahoma, United States The University of Tulsa, 1997.

Yoshida, Oka, Y.I., T., "Practical Estimation of Erosion Damage Caused by Solid Particle Impact . Part 2: Mechanical Properties of Materials Directly Associated with Erosion Damage", 16th International Conference on Wear of Materials, Wear, Vol. 259, pp. 102 – 109, 2005,.

Y. Yang, Z.G. Zhang, et al," Heat transfer properties of nanoparticle in fluid dispersions nanofluids in laminar flow", International Journal of Heat and Mass Transfer 48 ,1107–1116, 2005.

Zhang, Y.L., Mclaury, B.S. and Shirazi, S.A., "Improvements of Particle Near – Wall Velocity and Erosion Predictions Using a Commercial CFD Code", Journal of Fluids Engineering, Vol. 131 (3), pp. 0313031 – 0313039, 2009.

Zhang, Y.L., Reuterfors, E.P., Mclaury, B.S., Shirazi, S.A. and Rybicki, E.F., "Comparison of Computed and Measured Particle velocities and Erosion in Water and Air Flows", 16th International Conference on Wear of Materials ,Wear, Vol. 263, pp. 330 – 338, 2007A.

Zhang, Y.L., "Application and Improvement of Computational Fluid Dynamics (CFD) in Solid Particle Erosion Modeling", Ph.D. Thesis, Department of Mechanical Engineering, Oklahoma, United States ,The University of Tulsa, 2006B .